J Therm Anal Calorim (2012) 109:273–286
DOI 10.1007/s10973-011-1750-z

Influence of Sn on the hydration of tricalcium aluminate, $Ca_3Al_2O_6$

Nabajyoti Saikia · Shigeru Kato · Toshinori Kojima

Received: 12 May 2011 / Accepted: 15 June 2011 / Published online: 29 June 2011

Abstract Tricalcium aluminate ($Ca_3Al_2O_6$, C_3A) containing 0–5% of Sn was synthesized by solid-state method, and the products were characterized by XRD technique. Differential thermo-analytical technique (DTA) along with X-ray diffraction (XRD) analysis and scanning electron microscopy (SEM) were applied to study the hydration behaviour of different C_3A samples with and without the presence of gypsum. Results indicate that C_3A can accommodate small amount of Sn in its structure and remaining amount forms SnO_2. Hydration studies of the synthesized C_3A shows that the additions of 0.5 and 1% Sn increase and 2% Sn decrease the reactivity of C_3A at the initial period (<3 h) of hydration. Increasing additions of Sn also increase the amounts of amorphous phases and hexagonal calcium aluminate hydrates in the cement pastes. The stabilities of these hydration products also increase with increasing content of Sn in C_3A at the experimental conditions. The presence of Sn significantly changes the hydration of C_3A and gypsum solid mixture at the initial period of hydration by enhancing the formation of more amounts of AFt and AFm phases. However, at the later stage of hydration (on or after 3 days), the hydration products in C_3A and gypsum pastes with and without the presence of Sn are almost similar.

N. Saikia (✉)
Department of Civil Engineering and Architecture,
Instituto Superior Tecnico, Technical University of Lisbon,
Av. Rovisco Pais, 1049-001 Lisbon, Portugal
e-mail: saikianj@gmail.com

S. Kato · T. Kojima
Department of Materials and Life Sciences, Seikei University,
Kichijoji-kitamachi, Musashino-shi, Tokyo 180-8633, Japan

Keywords Tricalcium aluminate · Sn · Hydration · DTA · XRD

Introduction

Production of cement clinker is a high temperature process, where different constituent phases of cement are formed due to the reaction between calcium compounds like lime with a mixture of silicates and aluminates like clay, shale, sand etc. materials. The major constituents of cement clinker are tricalcium silicate, Ca_3SiO_5, C_3S (54–60%), dicalcium silicate, Ca_2SiO_4, C_2S (6.0–19.0%), tricalcium aluminate, $Ca_3Al_2O_6$, C_3A (1.6–13.3%) and tetracalcium aluminoferrite, $Ca_4Al_2Fe_2O_{10}$, C_4AF (7.0–12.9%). The amounts of different phases present in cement clinker may vary along with the variations in used raw materials, processing conditions etc. There is increasing interest in using different types of low-grade raw materials and fuels like fly ash, different types of slags, scrape tyre to prepare Portland cement clinker [1–4]. Introduction of these types of heterogeneous raw materials also modifies the properties of produced clinker by introducing different types of trace elements in the clinker [5]. These trace elements may form some new phases or may substitute the Ca, Si, Al, or Fe present in the different cement constituents, which may alter the properties of cement.

C_3A, one of the main phases of normal Portland cement clinker, plays an important role in the early stage of hydration process, and it is believed to be the responsible species for the setting and hardening behaviours of cement. The ionic substitution of this phase generally modifies its crystal structure as well as other properties.

Trace amount of tin (Sn) is generally found in raw feed and fuel during the preparation of Portland cement clinker

[5]. The non-volatile nature of Sn (boiling point approximately 2265 °C) suggests the possibility of presence of this element in cement clinker phases [5]. Tin oxide (SnO) or natural cassiterite melts at 1630 °C and sublimes between 1800 and 1900 °C. Recent application of different types of materials during the production of cement may increase the amount of Sn in cement clinker [6]. Our recent investigation also shows the presence of high amounts of Sn in the MSWI ash-based ecocement clinker [7].

In a review in 1995, it was reported that no report was available about the effect of Sn in clinker manufacture as well as in the hydration behaviour of cement and its constituents [5]. However, recently, a few studies were published to evaluate the effect of SnO_2 as a mineraliser in clinker production as well as the effectiveness of cement-based matrix to encapsulate Sn containing radioactive wastes [6, 8–13].

Addition of Sn during preparation of Portland cement clinker can improve the burnability of clinker raw mix [8, 14]. The C_3S can incorporate very little amounts of Sn in its structure but most amounts of SnO_2 form a solid solution with CaO. On the other hand, Sn is not detected in C_2S, the other silicate phase in clinker [9]. Addition of SnO_2 also changes the morphology of clinker phases [8, 9]. However, it is not clear whether C_3A, an important clinker mineral in Portland cement, can accommodate Sn in its structure or not.

Addition of 0.5% of SnO_2 in cement raw mix increases the rate of hydration and hardening process of resulting clinker [8]. The solubility of Sn(IV) in cementitious systems is dependent on the concentration of Ca in cement pore fluid [10]. At high Sn(IV) concentrations, Sn(IV) immobilization in hardened cement paste occurs due to the formation of $CaSn(OH)_2$ [11]. On the other hand, calcium silicate hydrate, major product in cement paste may not be the uptake-controlling phase for Sn immobilization [11]. It is speculated that Sn can interact with calcium sulpho aluminate-based products, ettringite during the hydration of cement [11]; however, further study is necessary to prove this hypothesis. On the other hand, $SnCl_2$ gets oxidized to $SnCl_4$ and forms $CaSn(OH)_6$ during hydration of this compound with NPC or NPC-blast furnace slag-based cement composite [12, 13].

As discussed above, the influence of Sn on the hydration of cement and its clinker phases, mainly C_3A, is not clear due to the limited amounts of information. By considering this gap, therefore, in this communication, we reported the influence of Sn on the hydration behaviour of C_3A.

Experimental

In traditional solid-state method, $CaCO_3$ and Al_2O_3 are generally used as raw materials to produce C_3A. However, several grinding and calcining steps are necessary to obtain the desired product. Moreover, the resulting product often contains appreciable amounts of secondary phases and unreacted compounds. Some other methods like wet chemical method, spray-drying method and solid-state method using some more reactive chemicals can also be applied to synthesize single phase C_3A. In this study, we chose solid-state method, where more reactive sources of aluminium and calcium, namely, nitrate salts of these elements are used. These reactive salts ensure rapid and complete reaction due to more favourable decomposition kinetics compared to their carbonate and oxide counterparts. Moreover, this method is similar to the conventional solid-state method.

The Sn-doped C_3A were prepared from mixtures of analytical grade $Ca(NO_3)_2{\cdot}4H_2O$, $Al(NO_3)_3{\cdot}9H_2O$, $SnCl_4{\cdot}5H_2O$ and SnO_2. The tin compounds were added in such a way that 0.5, 1, 2 and 5% of Sn (w/w) can be added with C_3A. As Sn is a non-volatile element, therefore, no Sn will be lost during heating stage, which is also observed in other studies [6, 7]. The SnO_2 was considered to clarify the any effect of chloride ion, if present in C_3A crystal during formation as well as hydration of Sn-doped C_3A, prepared using $SnCl_4{\cdot}5H_2O$. For each composition, the stoichiometric mixture was thoroughly ground in an agate mortar and mixed in a ball mill for 3 h. The mixtures were then initially heat-treated in a muffle furnace successively at 1000, 1100 and 1200 °C for 24 h at each temperature. The resulting white powder samples were then collected ground and characterized using powder X-ray diffraction (XRD) technique. After optimization of suitable temperature, which was 1200 °C in this case, more amounts of samples were prepared for further study.

To study the hydration behaviour, pastes were prepared by mixing powdered C_3A and C_3A–gypsum mixture with distilled deionized water, maintaining solid to water ratio of 1:1.4–1:1.5(g/mL) in a plastic container for about 5 min. For Sn containing mixes, slightly high amounts of water was necessary for making the cement pastes. The water requirement increased with increasing amount of Sn in C_3A. The airtight containers of the paste were then kept in desiccators at ambient temperature and allowed to hydrate up to 30 days. The hydration was stopped by grinding about 5 g of the pastes with an acetone:methanol (1:1) liquid mixture for ~5 min in a porcelain mortar. Hydrated products were then washed several times with the same liquid mixture and dried at 60 ± 5 °C for 2 h in an air-oven and stored in airtight containers and in desiccators.

The thermal curves (DTA) of the hydration products were taken in a thermo gravimetric apparatus (Shimadzo thermal analysis system, model TA-60WS). A total of ~20 mg of the samples were heated in an aluminium crucible in nitrogen atmosphere up to 1000 °C, maintaining 10 °C/m heating rate and using α-Al_2O_3 as the reference

material. The XRD patterns of the samples were recorded using Cu K_α radiation (Miniflex, MJ 14848 B01, Rigaku, Japan). Scanning electron micrographs (SEMs) of some of the hydrated samples were obtained using a scanning electron microscope (model JSM-5200; Jeol, Tokyo, Japan). Samples were prepared by sprinkling the prepared powder onto carbon paper placed on aluminium stubs followed by gold coating.

Results and discussion

Synthesis of C_3A

The XRD patterns of the C_3A containing different amounts of Sn as $SnCl_4{\cdot}5H_2O$, prepared at 1200 °C, are shown in Fig. 1. In the same figure, the XRD pattern of C_3A containing 2% Sn as SnO_2 is also presented.

All the samples contain C_3A as the major phase without showing any peaks of $C_{12}A_7$, which is generally observed as minor phase during preparation of C_3A. This phase is indicated by the characteristic diffraction peaks at $2\theta = 33.14°$, 47.55° and 59.15° corresponding to the main reflection, (440), (008) and (844), respectively.

The major XRD peaks corresponding to C_3A are shifted to lower angle due to incorporation of Sn in C_3A though the intensities and peak widths are not much affected due to the addition of Sn. The maximum shifting is observed for C_3A containing 1% Sn. However, at higher addition, C_3A peaks are again shifted into high angle. Table 1 shows the 2θ values observed for these peaks.

The XRD patterns of 2 and 5% Sn containing C_3A also exhibit two peaks at 2θ of 26.11° and 26.62°. The XRD pattern of C_3A containing 5% Sn also exhibits another peak at 33.93°. The appearance of these peaks suggests the presence of SnO_2 (JCPDS 21-1250) in C_3A samples. Phase pure SnO_2 exhibits two peaks at 26.62° and 33.93°. The peak position observed at 2θ around 26.11° in the XRD patterns of C_3A containing 2 and 5% Sn is possibly due to the doping of Ca in SnO_2. The XRD apparatus used in this study cannot detect crystalline components in a mixture with concentration less than 2%. Therefore, small amount of SnO_2 may be present in the C_3A samples containing 0.5 and 1% Sn too. The presence of SnO_2 peaks in the XRD spectra indicate that a part of the added Sn instead of being doped into C_3A crystal remained

Table 1 XRD peak positions of tricalcium aluminate for the reflections of (440), (008) and (844) planes

Composition	Positions of peaks due to reflection of planes		
	440	008	844
C_3A	33.25	47.67	59.30
C_3A–0.5%Sn	33.19	47.60	59.28
C_3A–1%Sn	33.04	47.47	59.11
C_3A–2%Sn	33.20	47.62	59.27
C_3A–5%Sn	33.21	47.63	59.28

Table 2 Intensity of C_3A peak observed at about 2θ of 33.2° in the XRD patterns of C_3A pastes containing different amounts of Sn hydrated for different time periods

Hydration time	Intensity/counts per sec			
	0	0.5	1.0	2.0
0 min	4210.7	4256.8	4215.1	4241.4
30 min	1170.0	903.3	950.0	1410
3 h	1123.3	726.7	736.7	936.6
1 day	900.0	653.3	630.0	633.3
3 day	806.7	593.3	610.3	613.3
7 day	575.0	590.7	600.0	605.3

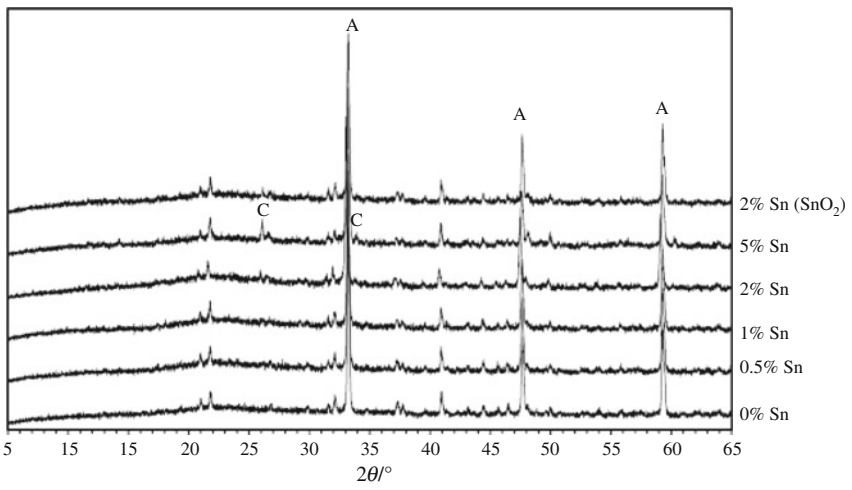

Fig. 1 XRD patterns of C_3A containing different amounts of Sn [*A* C_3A; *C* SnO_2]

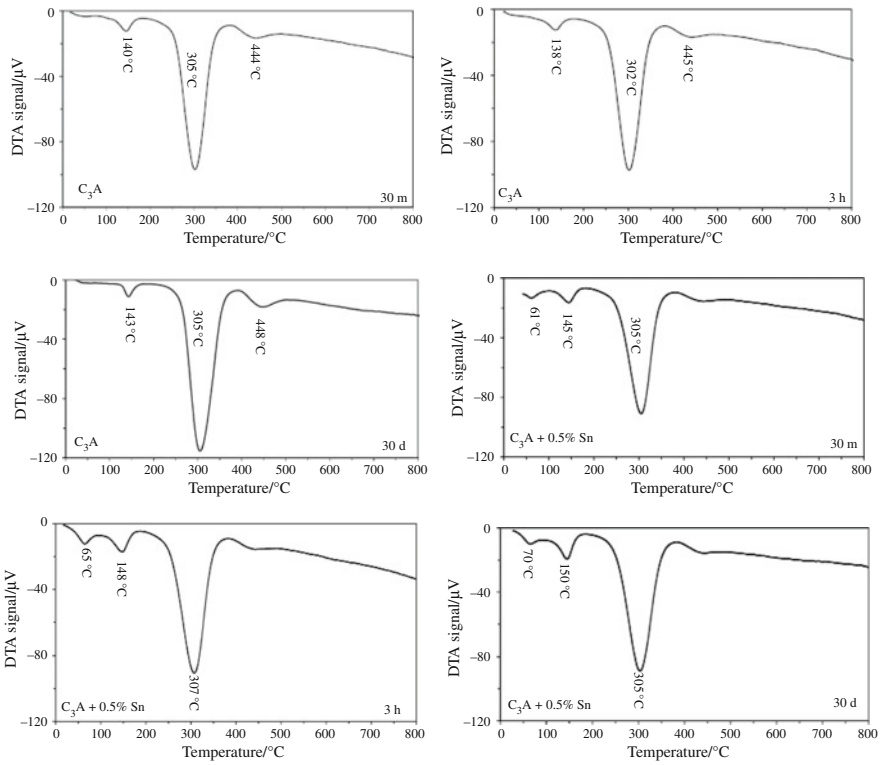

Fig. 2 Differential thermo-analytical patterns of C_3A pastes containing 0 and 0.5% Sn hydrated for different time periods

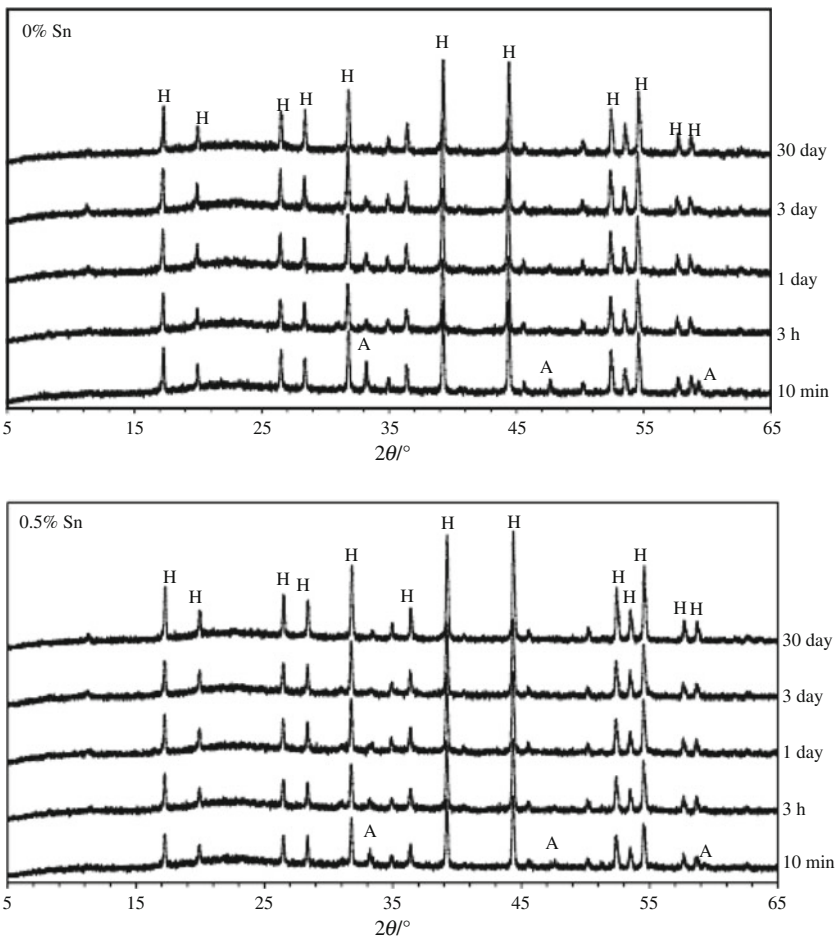

Fig. 3 XRD patterns of C_3A pastes containing 0 and 0.5% Sn, hydrated for different time periods [*A* C_3A; *H* hydrogarnet]

separated as SnO_2. It is possible that C_3A can accommodate small amount of Sn in its structure and remaining amount may prefer to stay as SnO_2 during formation of C_3A. The shifting of peak positions of C_3A synthesize in the presence of Sn might be due to the deformation of lattice parameters due to incorporation of Sn ions. The incorporation of foreign ions causes deformation of crystal lattice by increasing some interplanar spaces and decreasing some others. However, further study is necessary to confirm this observation. Earlier study also reported that most of SnO_2 present in clinker raw mix formed a solid solution with CaO [9].

The chemical analyses of different Sn containing C_3A show the presence of approximately same amount of Sn, as added before firing the raw mixture, which suggests that negligible amount of Sn is volatilized during the firing. The free lime contents of all these mixtures are very low (<0.5%); a decreasing trend of free lime content in C_3A was observed due to the increasing addition of Sn.

Hydration of C_3A

Effect of Sn on the reactivity of C_3A

The intensities of C_3A peak observed at about 2θ of 33.2° in the XRD patterns of C_3A paste containing different amounts of Sn, hydrated for different time periods, are presented in Table 2.

The peak intensity of C_3A in the pastes containing 0.5 and 1% of Sn is considerably lower, and the peak intensity of the paste containing 2% Sn is considerably higher than the corresponding peak intensity of undoped C_3A paste after 30 min of hydration. The intensities of C_3A peaks of all Sn containing hydrated pastes are lower than the similar peak corresponds for undoped C_3A paste on and after 3 h of hydration. However, the intensities of C_3A peaks in all the Sn containing compositions become almost similar to the undoped C_3A on 7 days of hydration. This indicates that the presence of Sn in C_3A increases the rate of

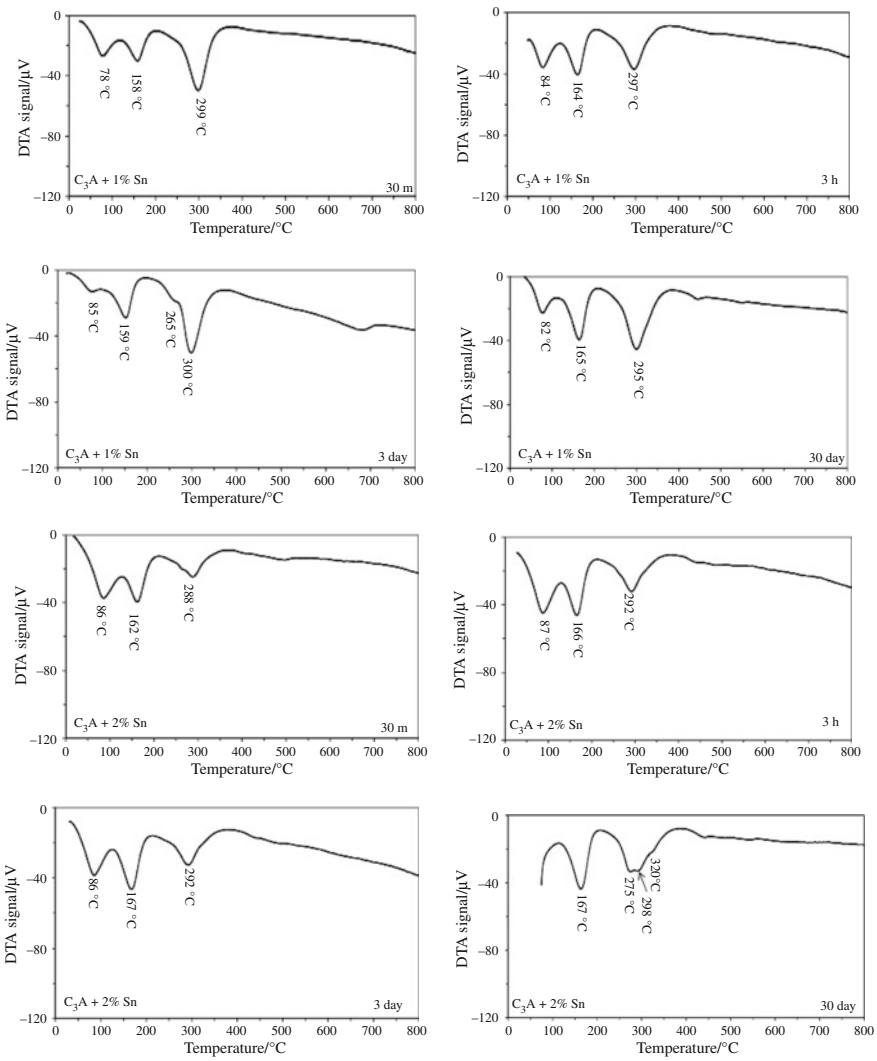

Fig. 4 Differential thermo-analytical patterns of C_3A pastes containing 1 and 2% Sn, hydrated for different time periods

hydration of C_3A at least up to 3 days of hydration; however, an initial dormant period is possibly existed during the hydration of C_3A paste containing 2% Sn. Thus, the content of Sn in C_3A may be a deciding factor as at higher content of Sn may reduce reactivity of C_3A at the early stage of hydration.

The higher reactivity of 0.5 and 1% Sn containing C_3A than normal C_3A at the early period of hydration is probably due to the doping of Sn in C_3A crystal. The rapid diffusion of water through Al_6O_8 rings due to the presence of large-sized Sn cation in C_3A crystal and/or strain in C_3A crystal due to the incorporation of large-sized Sn in crystallographic sites of C_3A may enhance the hydraulic reactivity of C_3A containing 0.5 and 1% Sn [15]. It was also proved in earlier observation that the small addition of SnO_2 in cement raw mix increased the rate of hydration and hardening process of resulting clinker [8]. On the other hand, presence of SnO_2 in 2% Sn containing C_3A paste may form a protective layer on the C_3A surfaces like many other elements due to the formation of some Sn containing compounds and inhibits the initial rate of hydration of C_3A. When this protective layer breaks or solubilises the hydration proceeds in a similar way like normal C_3A paste. The presence of several elements like Zn, Pb, Cd and Cu can lower the rate of hydration of cement pastes including C_3A by forming some protective layers on the unhydrated cement minerals [16–18]. The retardation of cement hydration is also dependent on the solubilities of the protective layer forming compounds, mainly metal hydroxides [19, 20].

Hydration of C_3A-H_2O

The DTA patterns of C_3A pastes containing 0 and 0.5% Sn, cured for 30-min, 3-h and 30-days, are presented in Fig. 2. The DTA patterns of both pastes exhibit a strong endotherm in the temperature range of 250–375 °C with a minimum at about 305 °C, due to formation of hydrogarnet, C_3AH_6 and another weak endotherm in the temperature range of 400–460 °C, due to the presence of $Ca(OH)_2$ and/or hydrogarnet in the hydration products. The DTA patterns of both pastes also exhibit a weak endotherm in the temperature range of 135–145 °C, due to the presence of

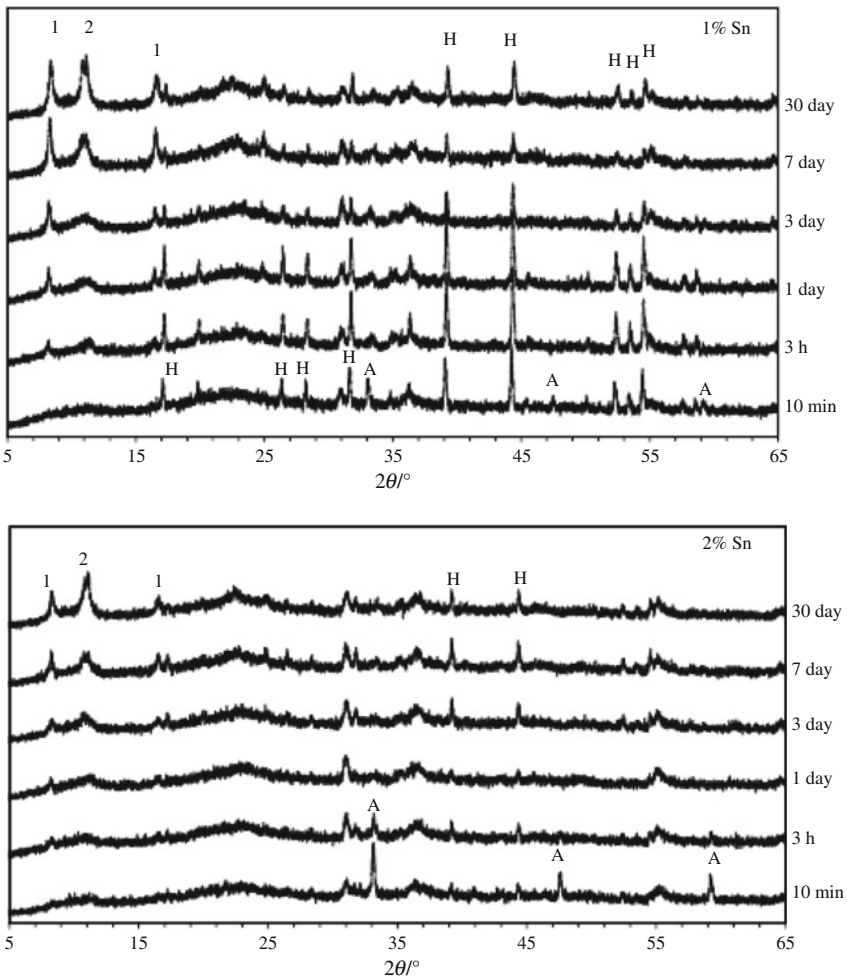

Fig. 5 XRD patterns of C_3A pastes containing 1 and 2% Sn, hydrated for different time periods [*1* C_2AH_8; *2* C_4AH_{13}; *A* C_3A; *H* hydrogarnet]

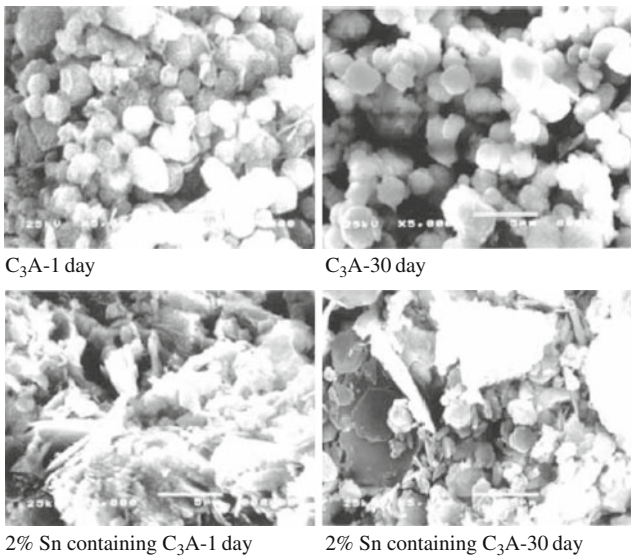

Fig. 6 Scanning electron micrographs of C_3A paste and C_3A paste containing 2% Sn, hydrated for 1 and 30 day

small amount of amorphous phase. The DTA patterns of C_3A pastes containing 0.5% Sn show another weak endotherm in the temperature range of 75–100 °C, possibly due to the presence of adsorbed water in some types of amorphous phases.

After 30 min of hydration, undoped C_3A paste shows the formation of cubic hydrogarnet, (C_3AH_6) as the major product with small amount of amorphous materials. The endotherm corresponds to the C_3AH_6 is gradually becoming stronger on prolonging the hydration time, which indicates the formation of more amounts of C_3AH_6 with progress of hydration. However, most of the C_3AH_6 are formed within 30 min of hydration of C_3A.

The endothermic minimum corresponding to amorphous phase is stronger and the endothermic minimum observed for C_3AH_6 is weaker in the DTA patterns of C_3A pastes containing 0.5% Sn, hydrated for different time periods than the equivalent endothermic minimum those observed in the corresponding DTA patterns of undoped C_3A paste,

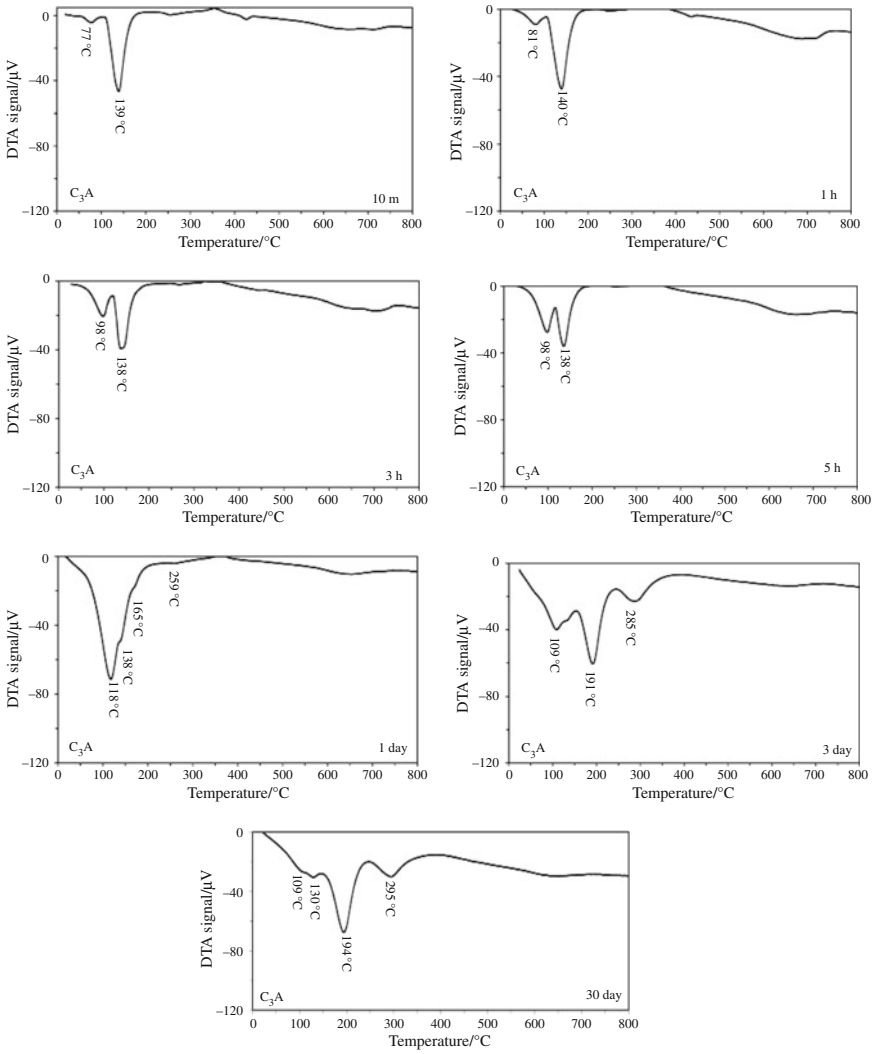

Fig. 7 Differential thermo-analytical patterns of C_3A + gypsum pastes, hydrated for different time period

which indicates the formation of more amounts of amorphous materials and lesser amounts of C_3AH_6 in C_3A pastes containing 0.5% Sn compared to undoped C_3A paste.

The XRD patterns of C_3A pastes containing 0 and 0.5% of Sn, cured for 30-min, 3 h, 1-, 3- and 30-days, are shown in Fig. 3. The XRD patterns of C_3A paste, obtained after 30 min of hydration, showed the presence of C_3AH_6 as the only hydration product along with strong peaks due to the presence of some amounts of unhydrated C_3A. The intensities of the peaks correspond to C_3AH_6 is increasing slightly with decreasing the intensities of C_3A peaks at the latter stages of hydration, indicating hydration of C_3A with prolonging the hydration time. The intensities of C_3AH_6 peaks observed in the XRD patterns of pastes of 0.5% Sn-doped C_3A obtained at different time intervals are almost similar to the corresponding peaks present in the XRD patterns of undoped C_3A pastes.

The doping of Sn in C_3A at 1 and 2% level changes the hydration behaviour of C_3A in a striking way. The DTA patterns of the cement pastes containing 1 and 2% Sn-doped C_3A are presented in Fig. 4. The position of 140–145 °C endothermic minimum as observed in the C_3A and 0.5% Sn-doped C_3A paste is shifted to higher temperature region with increasing hydration time as well as with increasing content of Sn in C_3A pastes. The intensity of this endotherm along with the intensity of endotherm observed in the 90–100 °C region in 1 and 2% Sn containing C_3A pastes are increasing, and the intensity of endotherm observed at 290–310 °C region is decreasing with increasing content of Sn in C_3A pastes. The strong endothermic minimum observed at 160 °C region for 1% Sn-doped C_3A and 165 °C region for 2% Sn-doped C_3A suggests the formation of some hexagonal hydrates like C_2AH_8 and C_4AH_{13} along with amorphous phases, during hydration of these pastes. A

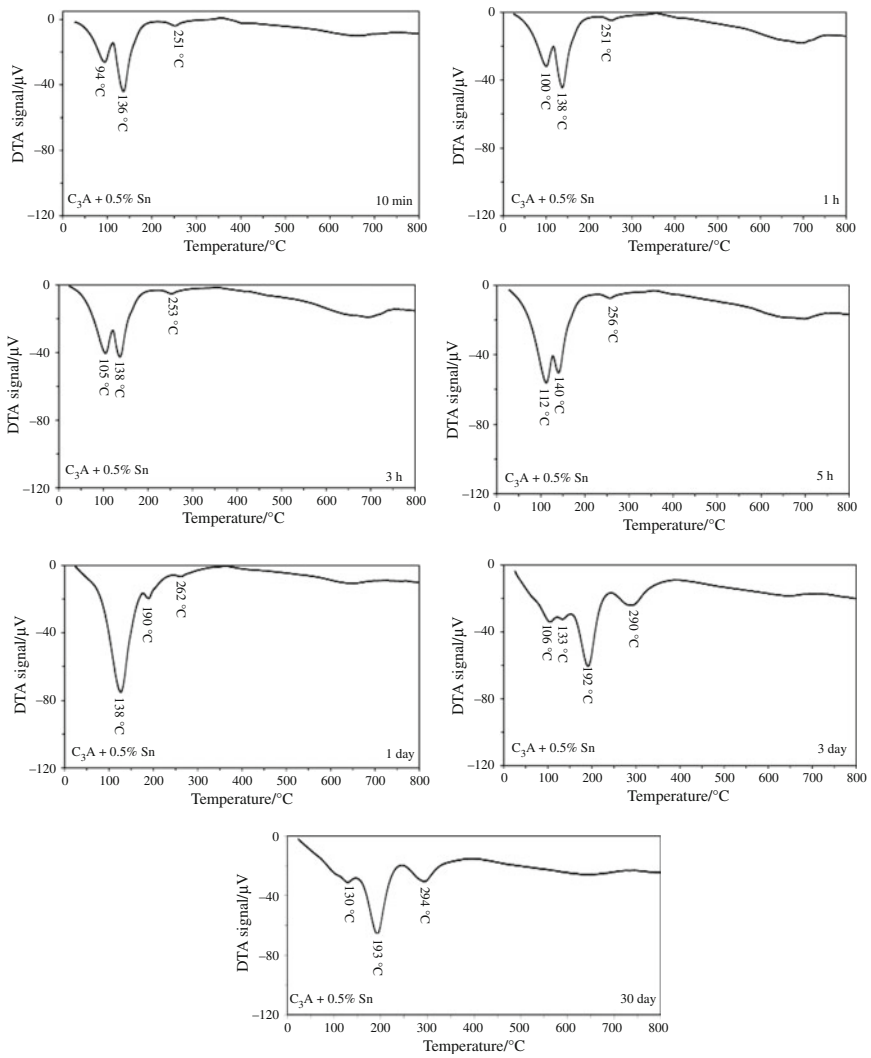

Fig. 8 Differential thermo-analytical patterns of C_3A + gypsum pastes containing 0.5% Sn, hydrated for different time period

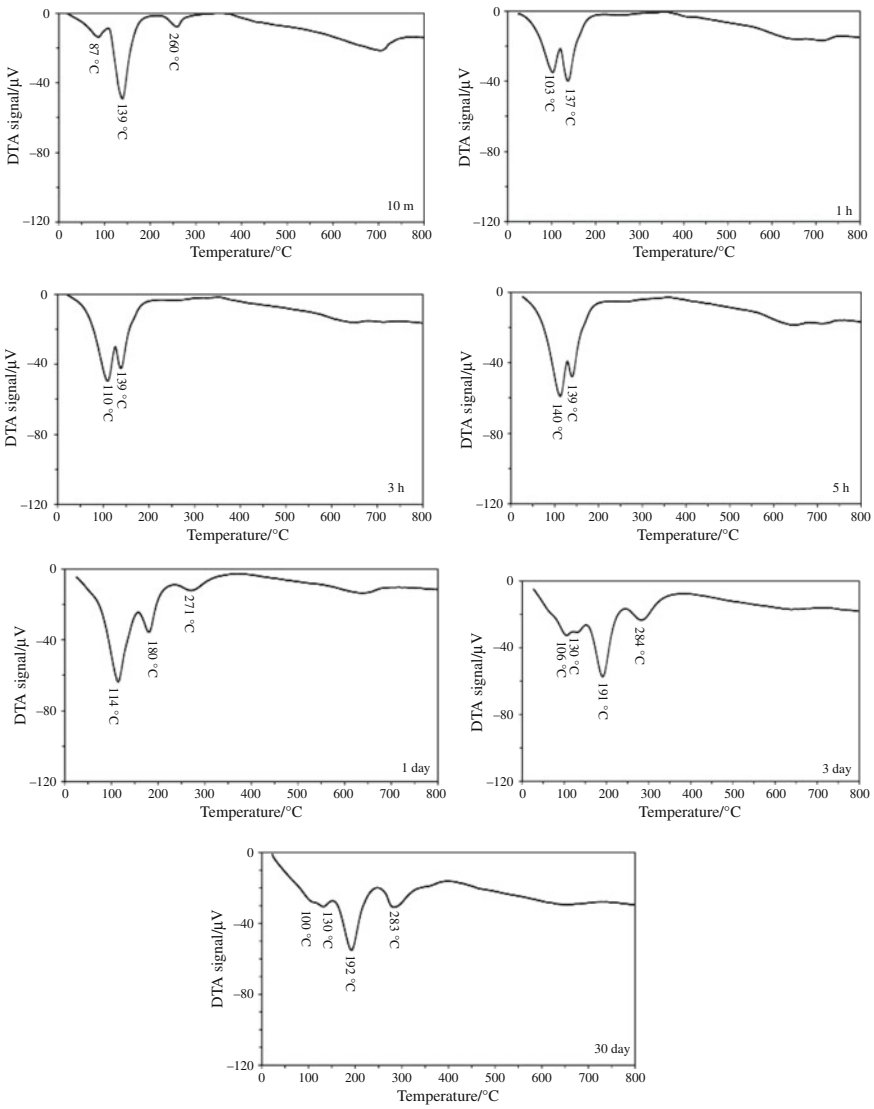

Fig. 9 Differential thermo-analytical patterns of C_3A + gypsum pastes containing 1% Sn hydrated for different time period

new endothermic hump, observed around 260–275 °C region in some C_3A pastes containing 1 and 2% Sn, suggests the formation of $CaSn(OH)_6$ during hydration [21]. However, gibbsite [$Al(OH)_3$] also exhibits an endotherm in this temperature region [22, 23].

In contrast to the XRD patterns of other two pastes, the XRD patterns of 1 and 2%-doped C_3A pastes diffuse in nature due to the presence of higher amount of amorphous phases (Fig. 5). The XRD patterns of 1 and 2% Sn containing C_3A pastes show some new peaks at 2θ value of 11.19°, 8.42° and 16.90° along with corresponding peaks of hydrogarnet, C_3AH_6. The peak observed at 2θ value of 11.19° is due to the presence of hexagonal hydrate with composition of C_4AH_{13}, and the two other peaks observed at 2θ values of 8.42° and 16.90° are attributed to another hexagonal hydrate phase, C_2AH_8. Appearance of two peaks or broad peak around 2θ value of 11.19° is probably due to the contamination of CO_3^{2-} in C_4AH_{13}. Another possibility is the presence of small amounts of hydrated Sn in C_4AH_{13}. The intensities of the peaks due to hexagonal hydrates in 1 and 2% Sn containing C_3A pastes are increasing with respect to increasing hydration time, indicating formation of more amounts of these materials with increasing hydration time.

Thus addition of Sn delays/inhibits the formation of C_3AH_6 phase by forming more amounts of amorphous phases as well as hexagonal hydrate phases. Increasing amounts of Sn content in C_3A also increases the amount of these phases (hexagonal hydrate and amorphous phases) in the hydrated paste. These hexagonal hydrates are also formed in the hydration of normal C_3A but rapidly converted into cubic hydrogarnet during its hydration [24]. The consequence of this transformation is the reduction in volume of paste, which leads to an increase in porosity and therefore low durability performance [25].

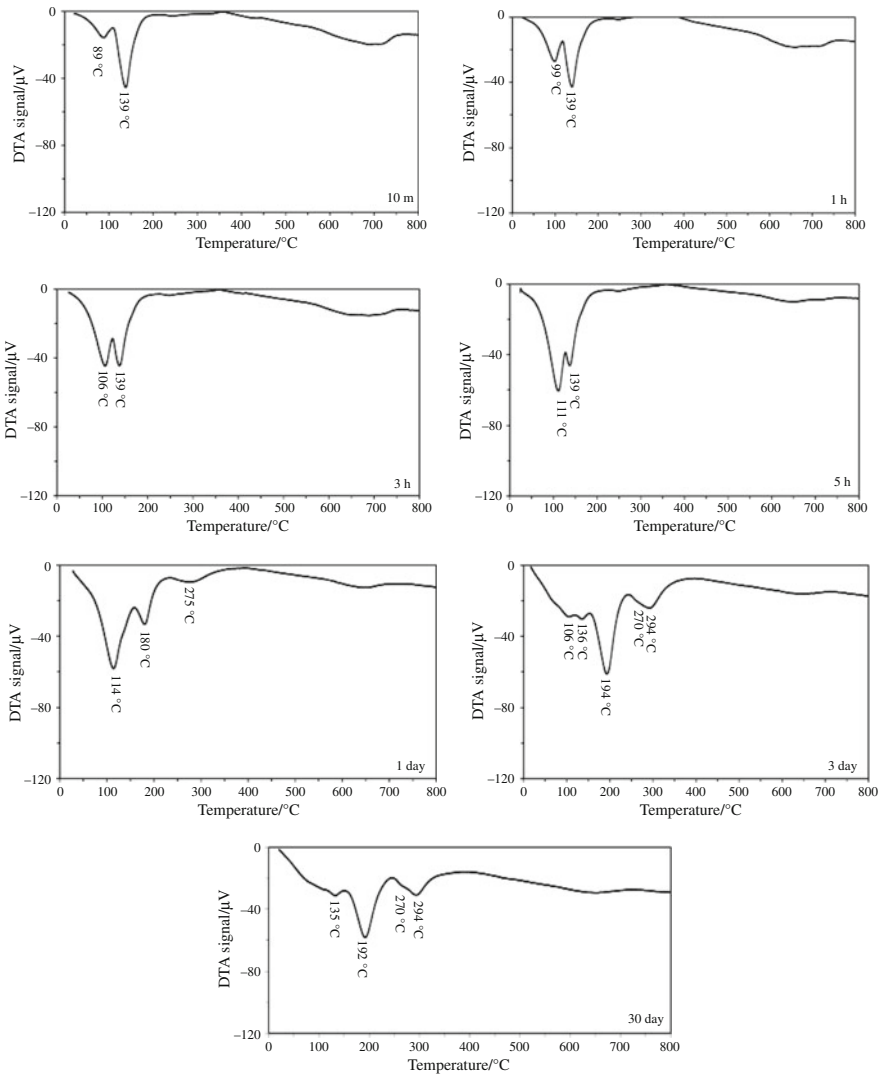

Fig. 10 Differential thermo-analytical patterns of C_3A + gypsum pastes containing 2% Sn hydrated for different time period

The SEMs of the C_3A and 2% Sn containing C_3A pastes hydrated for 1 and 30-day are presented in Fig. 6. The 1 and 30-day hydrated pastes of C_3A showed the presence of cubic hydrogarnet phase as the major hydration products. On the other hand, the 1-day hydration product of 2% Sn containing C_3A paste shows the presence of amorphous products as the major hydration product. After 30 days of hydration, the SEM of 2% Sn containing C_3A paste shows the presence of hexagonal hydrates, amorphous phases and cubic hydrogarnet as the hydration products.

The hydration of pure C_3A and formation of C_3AH_6 as observed in this investigation is similar to previous studies. The reaction of C_3A with water takes place rapidly and initially forms various amorphous gel which converts into hexagonal hydrates (C_2AH_8 and C_4AH_{19} or C_4AH_{13}) with prolonging of hydration reaction. However, these hexagonal phases are metastable and therefore transform into more stable cubic form, C_3AH_6 during the progress of reaction, depending on the reaction conditions. The transformation of hexagonal phase into cubic phase depends on temperature and water to C_3A ratio. In general, low temperature and low water to C_3A ratio enhance the stability of hexagonal phases [24, 25].

The hexagonal hydrates formed in cement hydration products are layered double hydroxide (LDH) type compounds. These compounds can take several types of anions like OH^-, SO_4^{2-}, CO_3^{2-} in its structure. This compound can incorporate several other oxyanions like $B(OH4)^-$, CrO_4^{2-}, MoO_4^{2-} and SeO_4^{2-} in its interlayer position [26, 27]. In cementitious environment with pH = 12–14 and Eh in the range of −400 to +200 mV, Sn may be present in its tetravalent form, Sn(IV), $Sn(OH)_5^-$ and $Sn(OH)_6^{2-}$ [28, 29]. Thus, there is a possibility of the formation of hexagonal hydrates containing $Sn(OH)_5^-$ and $Sn(OH)_6^{2-}$ during hydration of C_3A paste. The presence of $Sn(OH)_5^-$ and $Sn(OH)_6^{2-}$ in its structure possibly stabilize the hexagonal phase for long time. Another possibility is the formation of some insoluble Sn-

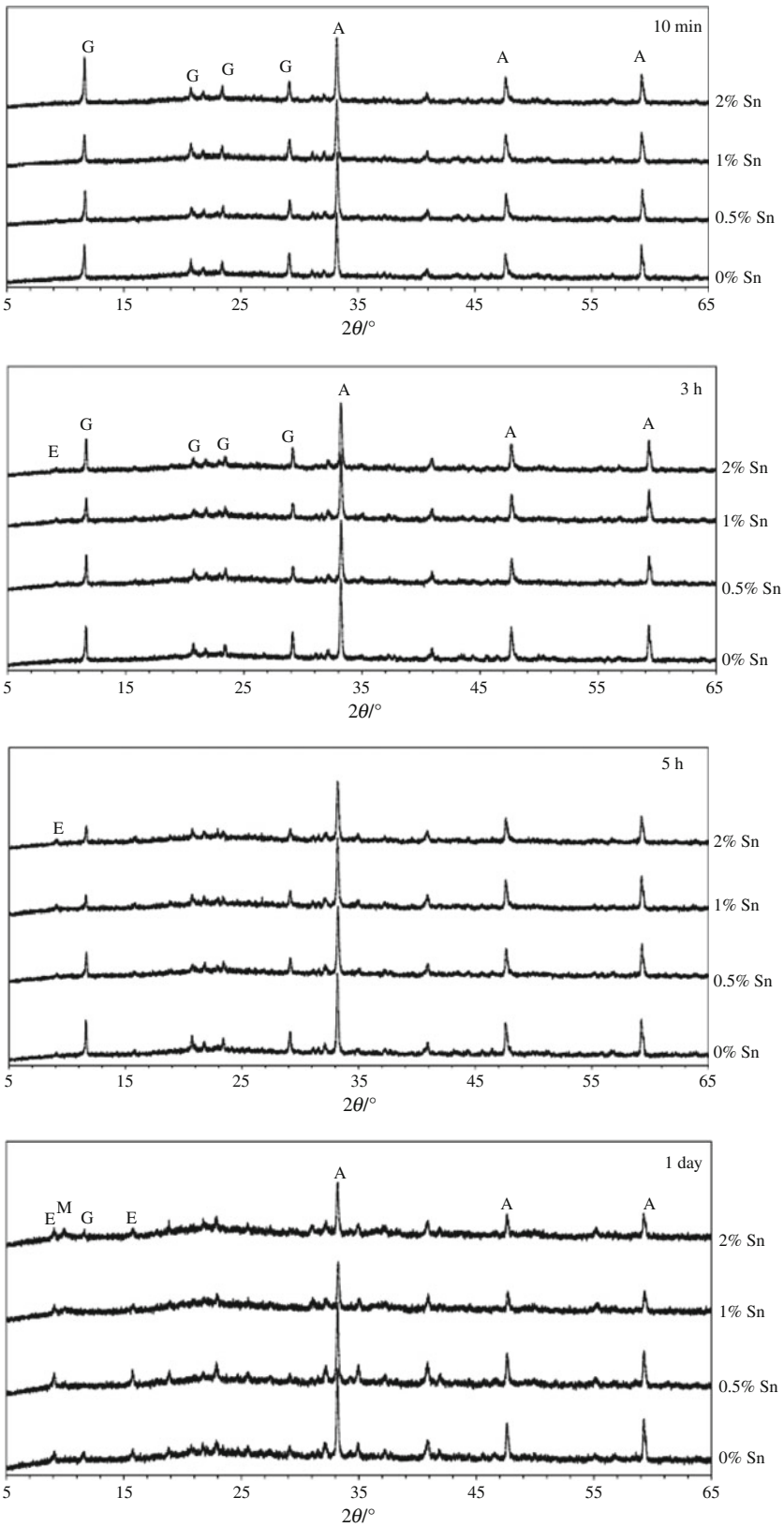

Fig. 11 XRD patterns of C_3A + gypsum paste containing various amounts of Sn and hydrated for different time periods [*A* C_3A; *E* ettringite; *G* gypsum; *M* monosulphoaluminate]

Fig. 11 continued

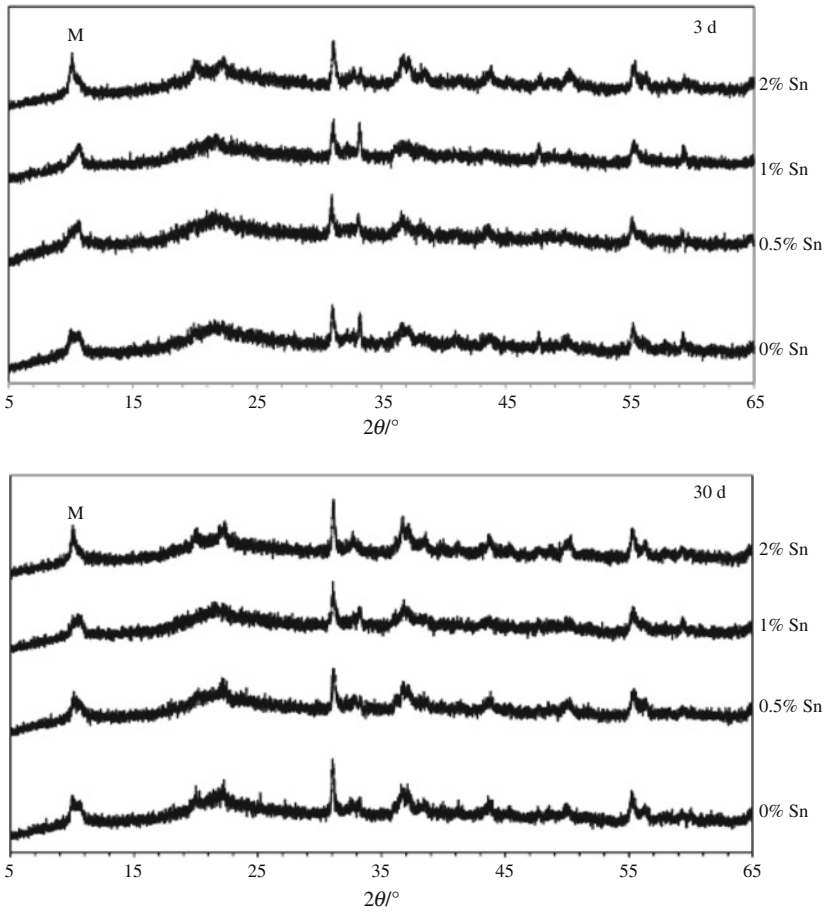

based compounds on the surfaces of hexagonal hydrates, which can inhibit the transformation of hexagonal hydrate into cubic hydrate during experimental hydration periods. The amorphous phase that observed in the XRD patterns may behave in this way.

The characterization of hydration products of C_3A pastes containing 1 and 2% Sn, where Sn is doped as SnO_2, indicates that the sources of Sn salt do not change the hydration behaviour of synthesise C_3A (figures are not presented here).

Hydration of C_3A-SO_4-H_2O

The DTA patterns of C_3A containing 0, 0.5, 1 and 2% of Sn hydrated in the presence of gypsum at different time periods are presented in Figs. 7, 8, 9 and 10. The DTA pattern of C_3A paste after 10 min of hydration shows a strong endothermic minimum at about 140 °C due to dehydration of gypsum and a weak endothermic minimum at about 77 °C, possibly due to loss of absorbed water. The endothermic minimum observed at 77 °C in the DTA curve of C_3A paste is shifted to 94 °C for C_3A paste containing 0.5% Sn and shifted to about 87 °C for other two C_3A pastes. The shifting of the temperature is possibly due to combined weight loss due to absorbed water as well as dehydration of ettringite, a hydration product and forms during hydration. The shifting of this endothermic minimum to higher temperature with increasing hydration time also supports this statement. The endothermic minimum due to gypsum in the DTA pattern of C_3A paste containing 0.5% of Sn is weaker than that observed in the DTA patterns of other C_3A pastes.

After 10 min of hydration, the endothermic minimum that corresponds to ettringite in the C_3A pastes containing 1 and 2% of Sn is stronger than the same observed for C_3A paste but weaker than the corresponding endothermic minimum observed in the C_3A paste containing 0.5% of Sn. This implies that the presence of Sn in C_3A increases the reactivity of C_3A and therefore increases the rate of formation of ettringite during hydration. As the C_3A containing 0.5% of Sn is more reactive than the C_3A as well as C_3A containing 1 and 2% of Sn (Table 2), therefore more amounts of ettringite are formed due to higher dissolution of C_3A at the early stage of hydration.

The endothermic minimum due to ettringite becomes stronger and due to gypsum becomes weaker in all the

C_3A pastes on prolonging the hydration time. The endothermic minimum corresponding to ettringite is also shifted to higher temperature with increasing hydration time. After 5 h of hydration, the strongest endothermic minimum due to ettringite was observed for the C_3A paste containing 2% Sn. The temperature of the endothermic minimum for ettringite is stabilized at about 115 °C for all the C_3A pastes.

The endothermic hump/minimum observed at about 190 °C in all types of C_3A pastes reveals the formation of monosulphoaluminate after 1 day of hydration. The DTA patterns of C_3A paste and C_3A paste containing 0.5% of Sn hydrated for 1 day show a hump and a weak endothermic minimum, respectively, at this temperature. On the other hand, corresponding endothermic minimum observed in the DTA patterns of C_3A pastes containing 1 and 2% Sn is almost similar but stronger than that observed in the DTA patterns of other two C_3A pastes. A new broad endotherm is observed in the all types of C_3A paste in the temperature range of 260–300 °C, due to the formation of some products including hydrogarnet, C_3AH_6. The position of this minimum shifted to lower temperature with increasing content of Sn in C_3A paste. The endothermic minimum for monosulphoaluminate and hydrogarnet getting stronger with increasing hydration time for all types of C_3A pastes. After 3 days of hydration, a distinct hump is observed at about 270 °C in the DTA pattern of C_3A paste containing 2% Sn and become visible at the latter stages of hydration, possibly due to the formation of $CaSn(OH)_6$. The DTA patterns of all the C_3A pastes after 30 days of hydration are almost similar to the corresponding DTA patterns of 3-day hydrated samples.

The XRD patterns of 10 min, 3, 5 h, 1, 3 and 30 day of the different C_3A pastes hydrated in the presence of gypsum are presented in Fig. 11. The XRD patterns also corroborate the findings observed in the DTA patterns. The peaks correspond to ettringite ($2\theta = 9.1$ and 15.2°) appears in the XRD patterns of C_3A pastes containing Sn after 3 h of hydration and in the C_3A paste after 5 h of hydration. Similarly, the peaks correspond to monosulphoaluminate ($2\theta = 9.8$ and 19.2°) in the C_3A pastes containing Sn and in the C_3A paste observed after 1 and 3 days of hydration, respectively. The intensities of peaks correspond to monosulphoaluminate also increase with increasing content of Sn in C_3A paste.

Conclusions

Following conclusions can be taken from the hydration study of C_3A paste containing 0, 0.5, 1 and 2% Sn with and without the presence of gypsum:

1. Tricalcium aluminate (C_3A) can possibly hold small amount of Sn in its structure and remaining amount may prefer to stay as SnO_2 during formation of C_3A.
2. The presence of Sn in C_3A increases the rate of hydration of C_3A; however, an initial dormant period is observed during the hydration of C_3A paste containing 2% Sn.
3. The hydration products of C_3A and C_3A containing 0.5% of Sn are almost similar at the investigated time periods. On the other hand, presence of 1 and 2% Sn in C_3A increases the amounts of hexagonal hydrates and amorphous phases and decreases the amounts of cubic phase in the hydrated pastes. The amounts of hexagonal hydrates and amorphous phases in the C_3A pastes increase with increasing concentration of Sn in C_3A.
4. The combined DTA and XRD analyses indicate that the presence of Sn during the hydration of C_3A increases the rates of formation of ettringite and monosulphoaluminate. The amount of monosulphoaluminate formed during early stage of hydration also increases with increasing content of Sn in C_3A.
5. The DTA patterns of C_3A pastes containing 1 and 2% Sn with and without the presence of SO_4^{2-} exhibit a weak endotherm at around 260–275 °C, possibly due to formation of $CaSn(OH)_6$.

Acknowledgements Authors are grateful to Ms. Rie Matsumoto for her technical assistance during the experiment.

References

1. Dawson B. Emerging technologies for utilizing wastes in cement production. World Cem. 1992;45:22–4.
2. Sprung S. Relieving the environment through the utilization of secondary raw materials. Zem-Kalk-Gips. 1992;45:213–21.
3. Blumentahl M. The use of scrap tyres in the US cement industry. World Cem. 1992;45:14–20.
4. Komljenovic M, Petrasinovic-Stojkanovic L, Bascarevic Z, Jovanovic N, Rosic A. Fly ash as the potential raw mixture component for Portland cement clinker synthesis. J Therm Anal Calorim. 2009;96:363–8.
5. Bhatty JI. Role of minor elements in cement manufacture and use, Research and Development Bulletin RD109T. Skokie, IL: Portland Cement Association; 1995.
6. Kolovos KG. Waste ammunition as secondary mineralizing raw material is Portland cement production. Cem Concr Compos. 2006;28:133–43.
7. Saikia N, Kato S, Kojima T. Production of cement clinker from municipal solid waste incineration (MSWI) fly ash. Waste Manag. 2007;27:1178–89.
8. Badanoiu A, Paceagiu J, Voicu G. Hydration and hardening processes of Portland cements obtained from clinkers mineralized with fluoride and oxides. J Therm Anal Calorim. 2011;103:879–88.
9. Kolovos K, Tsivilis S, Kakali G. SEM examination of clinkers containing foreign elements. Cem Concr Compos. 2005;27:163–70.
10. Lothenbach B, Ochs M, Hager D. Thermodynamic data for the solubility of tin (IV) in aqueous cementitious environment. Radiochim Acta. 2000;88:521.

11. Bonhoure I, Wieland E, Scheidegger A, Ochs M, Kunz D. EXAFS study of Sn (IV) immobilized by hardened cement paste and calcium silicate hydrates. Environ Sci Technol. 2003;37:2184–91.
12. Hill J, Sharp JH. Encapsulation of Sn(II) and Sn(IV) chlorides in composite cements. J Am Ceram Soc. 2005;88:560–5.
13. Hill J, Sharp JH. The hydration products of Portland cement in the presence of tin(II) chloride. Cem Concr Res. 2003;33:121–4.
14. Kolovos KG, Dousis G, Tsivilis S, Kakali G. The effect of SnO_2 on the burnability of raw meal, the structure and the properties of cement clinker. ZKG Int. 2005;25:81–7.
15. Prodjosantoso AK, Kennedy BJ, Hunter BA. Phase separation induced by hydration of the mixed Ca/Sr aluminates $Ca_{3-x}Sr_xAl_2O_3$: a crystallographic study. Cem Concr Res. 2002;32:647–55.
16. Chen QY, Tyrer M, Hills CD, Yang XM, Carey P. Immobilization of heavy metal in cement-based solidification/stabilization: a review. Waste Manag. 2009;29:390–403.
17. Qiao XC, Poon CS, Cheeseman CR. Investigation into the stabilization/solidification performance of Portland cement through cement clinker phases. J Hazard Mater. 2007;B 139:238–43.
18. Murat M, Sorrentino F. Effect of large additions of Cd, Pb, Cr, Zn to cement raw meal on the composition and the properties of the clinker and the cement. Cem Concr Res. 1996;26:377–85.
19. Poon CS, Peters DJ, Perry R, Barnes P, Barker AP. Mechanism of metal stabilization in cement based fixation processes. Sci Total Environ. 1985;41:55–63.
20. Poon CS, Clark AI, Perry R. Permeability study of the cement based solidification process for the disposal of hazardous wastes. Cem Concr Res. 1986;34:1907–18.
21. He ZQ, Li XH, Liu EH, Hou ZH, Deng LF, Hu CY. Preparation of calcium stannate by modified wet chemical method. J Cent South Univ Technol. 2003;10:195–7.
22. Nilforoushan MR, Talebian N. The hydration products of a refractory calcium aluminate cement at intermediate temperatures. Iran J Chem Eng. 2007;26:19–24.
23. Hidalgo A, García JL, Cruz Alonso M, Fernández L, Carmen A. Microstructure development in mixes of calcium aluminate cement with silica fume or fly ash. J Therm Anal Calorim. 2009;96:335–45.
24. Gartner EM, Young JF, Damidot DA, Jawed I. Hydration of Portland cement. In: Bensted J, Barnes P, editors. Structures and performance of cements. 2nd ed. London: Spon Press: Taylor& Francis Group; 2002. p. 57–113.
25. Ramachandran VS. Action of triethanolamine on the hydration of tricalcium aluminate. Cem Concr Res. 1973;3:41–54.
26. Zhang M, Reardon EJ. Removal of B, Cr, Mo and Se from wastewater by incorporation into hydrocalumite and ettringite. Environ Sci Technol. 2003;37:2947–52.
27. Saikia N, Kato S, Kojima T. Behaviour of B, Cr, Se, As, Pb, Cd and Mo present in waste leachates generated from combustion residues during the formation of ettringite. Environ Toxicol Chem. 2006;25:1710–9.
28. Brookins DG. Eh-pH diagrams for Geochemistry. Berlin: Springer-Verlag; 1988.
29. Amaya T, Chiba T, Suzuki K, Oda C, Yoshikawa H, Yui M. Solubility of Sn(IV) oxide in dilute $NaClO_4$ solution at ambient temperature. Mat Res Soc Symp Proc. 1997;465:751–8.